

# Intrinsic climate dependency of ecosystem light and water-use-efficiencies across Australian biomes

Hao Shi<sup>1</sup>, Longhui Li<sup>1</sup>, Derek Eamus<sup>1,2,3</sup>, James Cleverly<sup>1,2</sup>, Alfredo Huete<sup>1</sup>, Jason Beringer<sup>4</sup>, Qiang Yu<sup>1</sup>, Eva van Gorsel<sup>5</sup> and Lindsay Hutley<sup>6</sup>

<sup>1</sup> Plant Functional Biology and Climate Change Cluster, University of Technology, Sydney, NSW, Australia

<sup>2</sup> Australian Supersite Network, University of Technology, Sydney, NSW, Australia

<sup>3</sup> National Centre for Groundwater Research and Training, University of Technology, Sydney, NSW, Australia

<sup>4</sup> School of Geography & Environmental Science, Monash University, Clayton, Vic, Australia

<sup>5</sup> CSIRO Marine and Atmospheric Research, Canberra, ACT, Australia

<sup>6</sup> Research Institute for the Environment and Livelihoods, Charles Darwin University, Darwin, NT, Australia

E-mail: [Longhui.Li@uts.edu.au](mailto:Longhui.Li@uts.edu.au)


Received 11 February 2014, revised 19 August 2014

Accepted for publication 26 August 2014

Published 3 October 2014

## Abstract

The sensitivity of ecosystem gross primary production (GPP) to availability of water and photosynthetically active radiation (PAR) differs among biomes. Here we investigated variations of ecosystem light-use-efficiency (eLUE: GPP/PAR) and water-use-efficiency (eWUE: GPP/evapotranspiration) among seven Australian eddy covariance sites with differing annual precipitation, species composition and temperature. Changes to both eLUE and eWUE were primarily correlated with atmospheric vapor pressure deficit (VPD) at multiple temporal scales across biomes, with minor additional correlations observed with soil moisture and temperature. The effects of leaf area index on eLUE and eWUE were also relatively weak compared to VPD, indicating an intrinsic dependency of eLUE and eWUE on climate. Additionally, eLUE and eWUE were statistically different for biomes between summer and winter, except eWUE for savannas and the grassland. These findings will improve our understanding of how light- and water-use traits in Australian ecosystems may respond to climate change.

 Online supplementary data available from [stacks.iop.org/ERL/9/104002/mmedia](http://stacks.iop.org/ERL/9/104002/mmedia)

Keywords: ecosystem light- and water-use-efficiencies, temporal scales, biomes, climate, spatial pattern

## 1. Introduction

Climate imposes important but often contrasting limitations on productivity in most vegetated biomes (Churkina and Running 1998). Among climate factors, solar radiation

provides the energy source for photosynthesis, while water availability alters leaf-scale photosynthesis via modulations of plant stomatal conductance (Beer *et al* 2009) and canopy-scale photosynthesis via changes in leaf area index (Eamus *et al* 2001). Ecosystem light-use-efficiency (eLUE) and water-use-efficiency (eWUE) are two critical traits of terrestrial ecosystems that characterize the sensitivity of biomass production to solar irradiance and water supply (Beer *et al* 2007, Hu *et al* 2008, Ponton *et al* 2006, Turner *et al* 2003). eLUE and eWUE differ substantially in range and



Content from this work may be used under the terms of the Creative Commons Attribution 3.0 licence. Any further distribution of this work must maintain attribution to the author(s) and the title of the work, journal citation and DOI.

vary with environmental stress and vegetation structure within and across biomes (Farquhar *et al* 1989, Law *et al* 2002, Schwalm *et al* 2006). The values of both eLUE and eWUE exhibit time-scale dependence in the sense that their primary environmental controls vary temporally (Campos *et al* 2013, Schwalm *et al* 2006, Turner *et al* 2003).

Historically, eLUE ( $\epsilon$ ) has been defined as the ratio of net primary production (NPP, aboveground or total,  $\epsilon_n$ ) or gross primary production (GPP,  $\epsilon_g$ ) to incident photosynthetically active radiation (PAR) or absorbed PAR (APAR) (Gower *et al* 1999). Based upon evolutionary and physiological theory,  $\epsilon_n$  and  $\epsilon_g$  are expected to converge across biomes (Goetz and Prince 1999). However, values of each are dependent on plant function type (Gower *et al* 1999, Schwalm *et al* 2006, Turner *et al* 2003). The biophysical, biochemical and meteorological controls of eLUE among biomes at multiple temporal time-scales are not well understood, resulting in imprecise estimates of NPP and GPP and uncertainties in the responses of eLUE to climate change (Kanniah *et al* 2011). For example, daily  $\epsilon_g$  decreased with increasing APAR but was poorly correlated with vapor pressure deficit (VPD) or air temperature ( $T_a$ ), while the relative values of  $\epsilon_g$  across biomes were influenced by relative nitrogen availability (Turner *et al* 2003). In contrast, Schwalm *et al* (2006) observed that changes in daily  $\epsilon_g$  were driven by variation in light and temperature with no correlation to water availability or foliar nitrogen, while annual  $\epsilon_g$  varied across biomes as a function of mean annual temperature (MAT) and leaf area index (LAI). Additionally, annual  $\epsilon_g$  can increase with increasing total annual precipitation and decreasing potential evapotranspiration (Polley *et al* 2011) or MAT (Lafont *et al* 2002).

eWUE reflects a trade-off between carbon gain and water loss from leaves and ecosystems (Baldocchi 1994), and is important for ecosystem productivity and resilience (Campos *et al* 2013, Huxman *et al* 2004). At the leaf-scale, eWUE is expressed as the ratio of net photosynthesis to transpiration but at the ecosystem-scale, eWUE is defined as the ratio of either NEE or GPP to ET or canopy transpiration (Beer *et al* 2009, Niu *et al* 2011). To quantify the role of water limitation on above-ground NPP, rain-use-efficiency (RUE, the ratio of above-ground NPP to rainfall) is widely used (Huxman *et al* 2004). Alternatively, inherent water-use-efficiency (IWUE,  $GPP \cdot VPD/ET$ ) can be used to normalize the effect of VPD on ET (Beer *et al* 2009, Eamus *et al* 2013). Daily eWUE is negatively correlated with VPD during the time of peak GPP activity (Ponton *et al* 2006) and so is monthly eWUE across a large range of biomes (Law *et al* 2002). In contrast, annual eWUE tends to be similar across biomes except for tundra vegetation (Law *et al* 2002). Across a grassland transect in China, LAI is considered as the primary determinant of seasonal eWUE (Hu *et al* 2008). Annual eWUE of grasslands may decrease (Li *et al* 2008) or increase (Niu *et al* 2011) with increasing annual precipitation whilst eWUE may differ between wet and dry years (Campos *et al* 2013, Huxman *et al* 2004) or wet and dry seasons (Eamus *et al* 2013), and varies with soil moisture and LAI (Beer *et al* 2009).

The lack of consensus on the relative importance of different controlling factors of eLUE and eWUE across biomes at multiple temporal scales reflects the complexity of interactions between terrestrial ecosystems and climate. Therefore, a key issue to resolve is the relationships of eLUE and eWUE to climatic drivers. The eddy covariance (EC) technique provides an opportunity to examine the potential relationships due to simultaneous measurements of solar radiation, carbon and water fluxes, VPD and soil water content (SWC), thereby generating an extensive time series of eLUE and eWUE from hourly to multi-annual time-scales. Concurrent measurement of meteorological variables with fluxes can be used to quantify limitations on eLUE and eWUE and the interaction of climate variables as determinants of eLUE and eWUE. Thus, the current study used EC data from seven contrasting ecosystems in Australia for examining the magnitude, spatial patterns, and environmental regulation of eLUE and eWUE at multiple time-scales (hourly, daily, eight-day, monthly, and yearly). These seven EC sites encompass a range of biomes along a large precipitation, species compositional and temperature gradient, thereby providing further insights into coupling between ecosystems and climate. We aimed to identify variations in eLUE and eWUE of Australian major ecosystems over different time-scales and their key climatic drivers among biomes. This will allow for a better understanding of the coupling of carbon and water cycles and the effects of climate change on ecosystem carbon budgets and water use.

## 2. Methods

### 2.1. Sites and data processing

Seven sites were selected for this study in Australia. Individual site names, details, statistics and plots are given in the supplementary information (see supplementary information available at [stacks.iop.org/ERL/9/104002/mmedia](http://stacks.iop.org/ERL/9/104002/mmedia)). These sites include four contrasting savannas (Savn, AU-Ade, AU-Asm, AU-Dry and AU-How sites), two different evergreen broadleaf forests (EBF, AU-Tum and AU-Wac sites), and one grassland (Grass, AU-Stp site) (supplementary table S1; supplementary figure S1). Bioclimatic classifications of these sites range from tropical wet-dry in northern Australia, through tropical semi-arid in central Australia to cool temperate mesic in southeastern. Mean annual precipitation is smallest in central Australia and largest in far northern monsoonal Australia. All sites show seasonal patterns in precipitation, temperature and VPD that interact with large fluctuations in water availability. Seasonal variability in temperature and PAR was larger at the two forests in southeastern Australia than at the grassland and savanna sites. Conversely, seasonal variability in VPD and rainfall was larger in the northern and central sites, where a distinct dry season occurs during Australian winter (supplementary figure S1).

At each site, LAI data were derived from the space-borne MODIS (Moderate Resolution Imaging Spectroradiometer)

sensor (500 m spatial resolution and eight day temporal resolution). The MODIS images are spatially similar to the footprint size of the EC data used. A central 3×3 window was used to extract the flux tower LAI time series. This sampling strategy can effectively reduce the error due to the scale mismatch between the tower footprint and MODIS pixels (Rahman *et al* 2005, Xiao *et al* 2005). Then the LAI data series were smoothed using the TIMESAT tool (Jönsson and Eklundh 2004). Mean maximum LAI ( $LAI_{max}$ ) for each site were aggregated at eight-day, monthly and yearly scales. Half-hourly meteorological data, water and CO<sub>2</sub> fluxes were measured using an EC system and associated meteorological sensors installed at each site. All data were processed through OzFlux standard methods (see supplementary information).

## 2.2. Wavelet aggregation method

Half-hourly eLUE and eWUE were defined as ratios of GPP to PAR and GPP to ET, respectively. For eLUE, using incident PAR as the denominator instead of APAR can couple carbon and energy budgets directly at the ecosystem level rather than merely focusing on the biological mechanisms that drive photosynthesis (Schwalm *et al* 2006). When large disturbances occurred (for example, fire or extensive insect-induced defoliation), flux and LAI data were excluded from all analyses to minimize the introduction of bias arising from the inclusion of short-term episodic large-scale fluctuations in these data. To analyze multi-scale interactions between eLUE/eWUE and forcing variables, measured carbon and water fluxes, meteorological variables, SWC and LAI were resolved using the wavelet transformation (Ding *et al* 2013, Stoy *et al* 2005, Torrence and Compo 1998). The wavelet transformation can be used to analyze time series such as EC fluxes (Scanlon and Albertson 2001) that contain non-stationary power at different frequencies (Daubechies 1990). Here a continuous wavelet transformation with the Morlet basis was employed. Half-hourly carbon and water fluxes and environmental factors were transformed, reconstructed and then aggregated at hourly, daily, eight-day, monthly, seasonal and yearly time-scales, respectively. eLUE and eWUE were concurrently calculated at each time-scale. The detailed description of the Morlet wavelet transformation and an example of the reconstruction at the Howard Springs site were given in supplementary material (supplementary figure S2).

## 3. Results

### 3.1. GPP responses to PAR and ET

Figure 1 shows the multi-temporal (i.e. at daily to yearly time-scales) responses of GPP to variations in PAR and ET across the various ecosystems. GPP and PAR were significantly correlated only at the two temperate forest sites ( $R^2=0.88-0.97$ ,  $p<0.001$  and  $R^2=0.67-0.98$ ,  $p<0.001$  at AU-Tum and AU-Wac, respectively) (figure 1). Generally, GPP exhibited a significant linear correlation with ET ( $R^2$  from 0.48 to 0.96,  $p<0.001$ ) at all sites across daily to

monthly time-scales. Across the three biomes, average eLUE and eWUE were largest in forests, intermediate in savannas, and smallest in the grassland. Among the savannas, eLUE and eWUE were largest at AU-How and AU-Ade (tropical savannas) and smallest at AU-Asm (semi-arid savanna).

### 3.2. Relationships of eLUE and eWUE with climate

eLUE was significantly correlated with air temperature and PAR, and eWUE was significantly correlated with PAR. However, these correlations across biomes became much weaker at shorter time-scales, especially at the hourly time-scale and in the summer when light is less limiting (table 1). PAR explained less variation in eLUE than VPD at all time-scales, and air temperature was less correlated with eWUE than VPD at all time-scales except the hourly time-scale. Henceforth, of climate factors we mainly focus on the relationships between eLUE/eWUE and VPD, but this does not mean the effects of PAR on eLUE and air temperature on eWUE were not important. Across all sites, eLUE and eWUE followed a negative logarithmic relationship with VPD (table 1; figure 2). The goodness-of-fit increased as the time-scale increased. However, within a given ecosystem, a significant relationship between eLUE or eWUE and meteorology was, on occasion, absent. For example, at the AU-How site, eWUE was very weakly or not correlated with VPD (figure 2). Likewise at the AU-Asm site, eLUE was very weakly or not correlated with VPD (figure 2). This suggests that the factors driving eLUE and eWUE can differ within and across biomes.

### 3.3. Relationships of eLUE and eWUE to SWC and LAI

Significant positive correlations between eLUE/eWUE and SWC were observed across all time-scales (table 1; figure 3). The strength of these correlations increased with increasing time-scale. SWC showed a slightly better relationship with eLUE at hourly time-scale than VPD (table 1), while at other time-scales, the influence of SWC was consistently and slightly weaker than VPD. Across all time-scales, SWC was less correlated with eWUE than VPD. Specifically, SWC explained much less compared to VPD in variation of eLUE in summer. Considering the seven ecosystems together, a spatial pattern emerged whereby ecosystems with high annual average SWC also had large eLUE and eWUE. This was consistent with the response of eLUE/eWUE to VPD because of the inverse relationship between SWC and VPD. However, the relationships between eLUE/eWUE and SWC varied from site to site. Notably, at the AU-How site, eLUE increased with SWC whereas eWUE appeared to decrease as SWC increased (figure 3).

There were significant positive correlations between eLUE or eWUE and  $LAI_{max}$  at eight-day, monthly and annual time-scales (table 1; supplementary figure S3). These relationships were much weaker than those between eLUE/eWUE and VPD. Specifically, in winter, eLUE and eWUE were moderately or weakly correlated with  $LAI_{max}$ . In

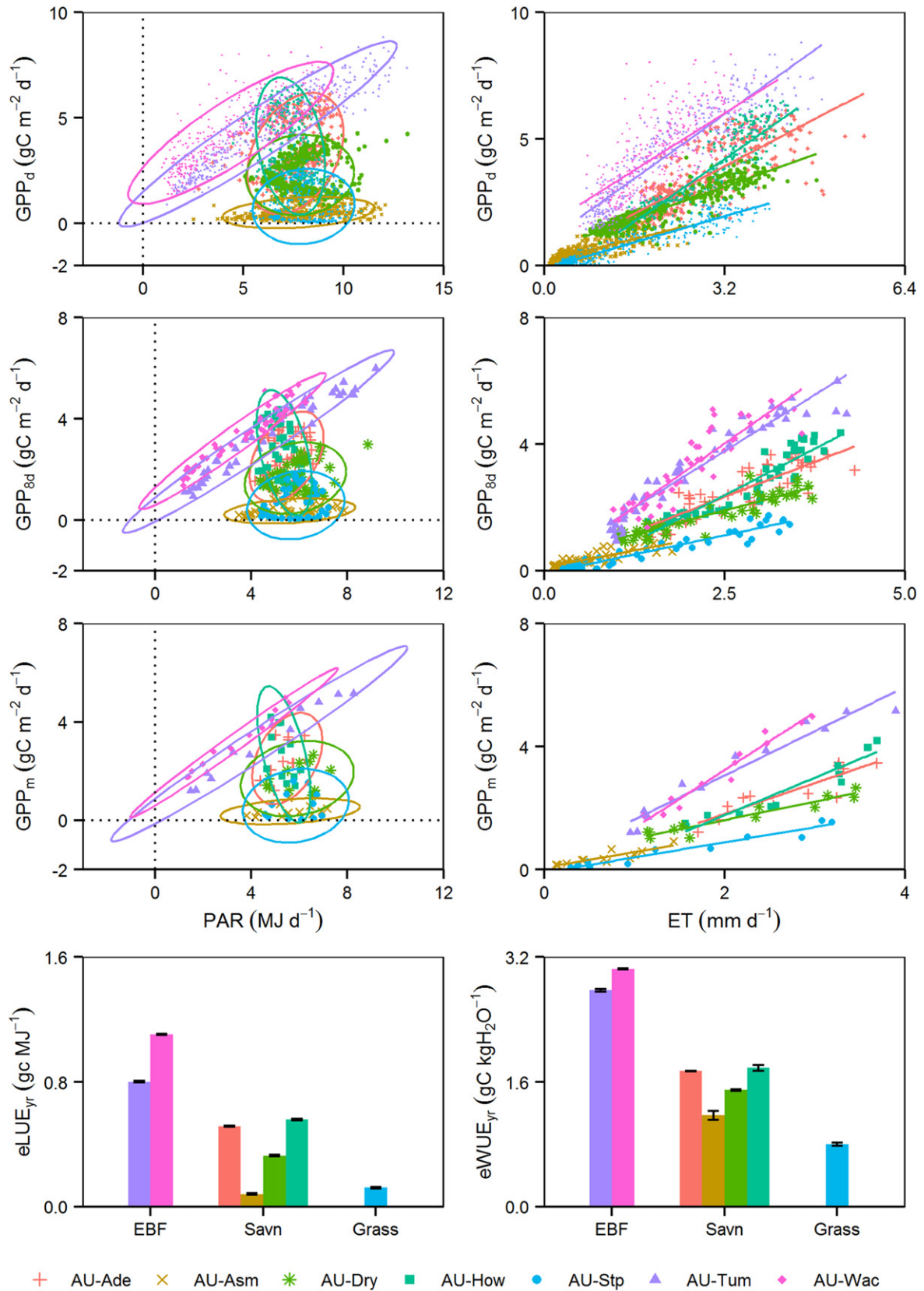


**Figure 1.** Relationships between (left) daily (GPP<sub>d</sub>), eight day (GPP<sub>8d</sub>), monthly (GPP<sub>m</sub>) GPP and PAR and between (right) GPP and ET for seven sites. Ellipses (left) indicate 95% confidence boundaries of GPP. Bars indicate annual standard deviations of eLUE or eWUE at each site. Also shown is the linear fit between GPP and ET (right). Annual eLUE(eLUE<sub>yr</sub>) and eWUE(eWUE<sub>yr</sub>) were calculated from annual GPP, PAR and ET.

**Table 1.** Coefficients of determination ( $R^2$ ) between LUE, WUE and  $T_a$ , PAR, VPD, SWC or  $LAI_{max}$  by logarithmic/exponential (Log/exp) and linear (Lin) fitting, respectively. \*\*\*, \*\*, \*, and NULL indicates significant relationship at  $p < 0.001$ , 0.01, 0.05 and not significant, respectively. Monthly(S) and Monthly(W) indicate monthly variables in summer (December, January, and February) and winter (June, January, and August).

Scale	Hourly		Daily		Eight-day		Monthly		Monthly(S)		Monthly(W)		Annual		
	Model	Log/exp	Lin	Log/exp	Lin	Log/exp	Lin	Log/exp	Lin	Log/exp	Lin	Log/exp	Lin	Log/exp	Lin
eLUE	$T_a$	0.34***	0.35***	0.41***	0.41***	0.43***	0.43***	0.44***	0.44***	0.38**	0.39**	0.52***	0.51**	0.59*	0.56
	PAR	0.20***	0.21***	0.52***	0.43***	0.46***	0.39***	0.46***	0.41***	0.40**	0.35**	0.77***	0.70***	0.82**	0.84**
	VPD	0.43***	0.34***	0.71***	0.62***	0.76***	0.71***	0.78***	0.75***	0.90***	0.83***	0.76***	0.74***	0.89**	0.94***
	SWC	0.59***	0.49***	0.63***	0.67***	0.63***	0.74***	0.64***	0.76***	0.63***	0.61***	0.65***	0.84***	0.70*	0.84**
	$LAI_{max}$					0.48***	0.33***	0.53***	0.38***	0.81***	0.58***	0.36**	0.20*	0.83**	0.68*
eWUE	$T_a$	0.52***	0.52***	0.62***	0.63***	0.62***	0.65***	0.64***	0.67***	0.65***	0.67***	0.63***	0.59***	0.75*	0.71*
	PAR	0.05***	0.11***	0.51***	0.46***	0.44***	0.41***	0.46***	0.44***	0.22*	0.19*	0.73***	0.69***	0.82**	0.85**
	VPD	0.49***	0.34***	0.71***	0.57***	0.74***	0.65***	0.78***	0.72***	0.83***	0.69***	0.79***	0.78***	0.95***	0.96***
	SWC	0.44***	0.45***	0.50***	0.56***	0.53***	0.62***	0.55***	0.66***	0.51***	0.60***	0.60***	0.77***	0.70*	0.81**
	$LAI_{max}$					0.50***	0.47***	0.55***	0.52***	0.82***	0.73***	0.49***	0.36**	0.84**	0.80**



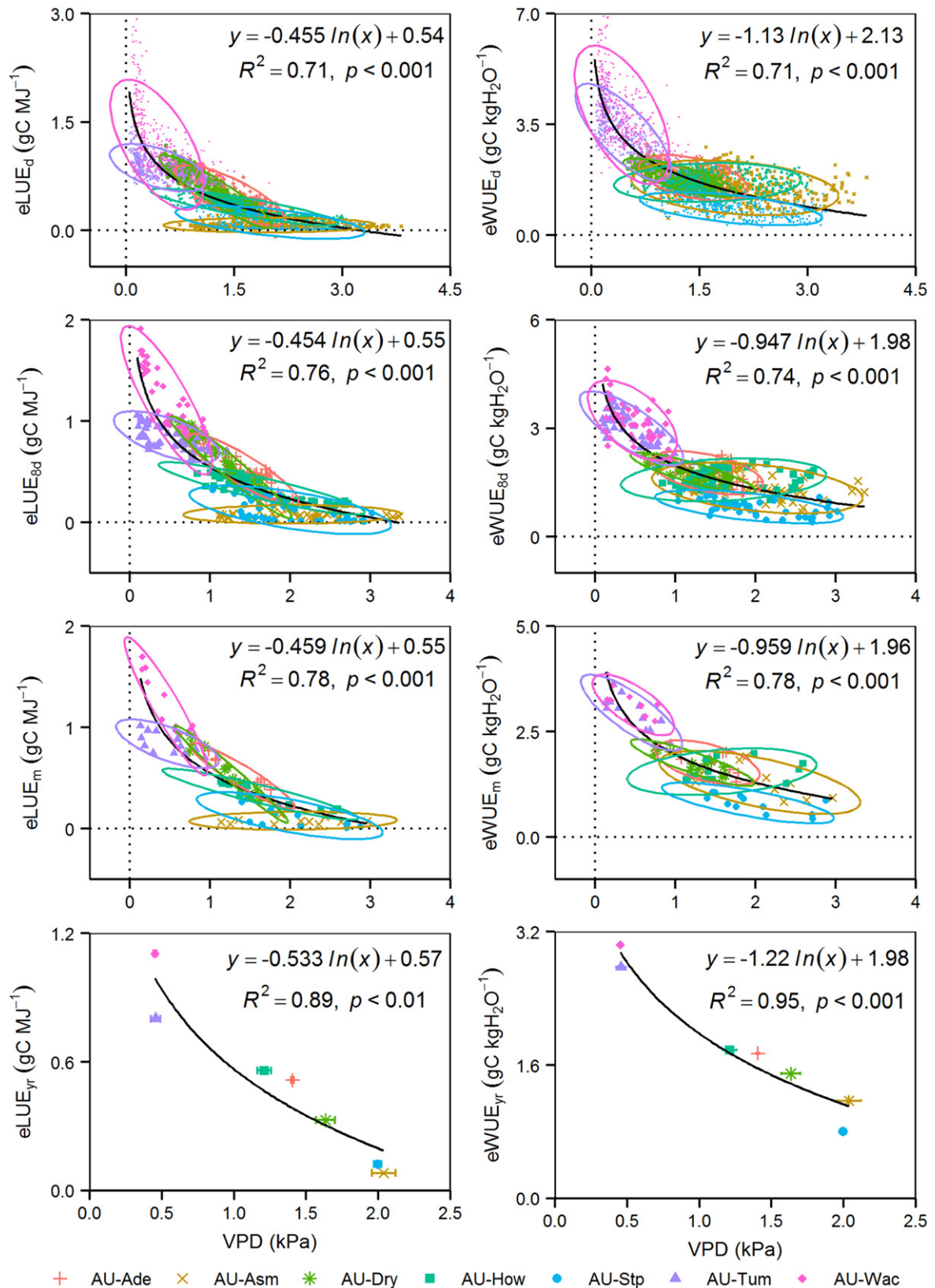


**Figure 2.** Relationships between (left) daily (eLUE<sub>d</sub>), eight day (eLUE<sub>8d</sub>), monthly (eLUE<sub>m</sub>) eLUE and VPD and between (right) daily (eWUE<sub>d</sub>), eight day (eWUE<sub>8d</sub>), monthly (eWUE<sub>m</sub>) eWUE and VPD for seven sites. Ellipses indicate 95% confidence boundaries of eLUE and eWUE. Bars indicate annual standard deviations of eLUE, eWUE or VPD at each site. Also shown are logarithmically fitted functions, coefficients of determination ( $R^2$ ) and  $p$  values.

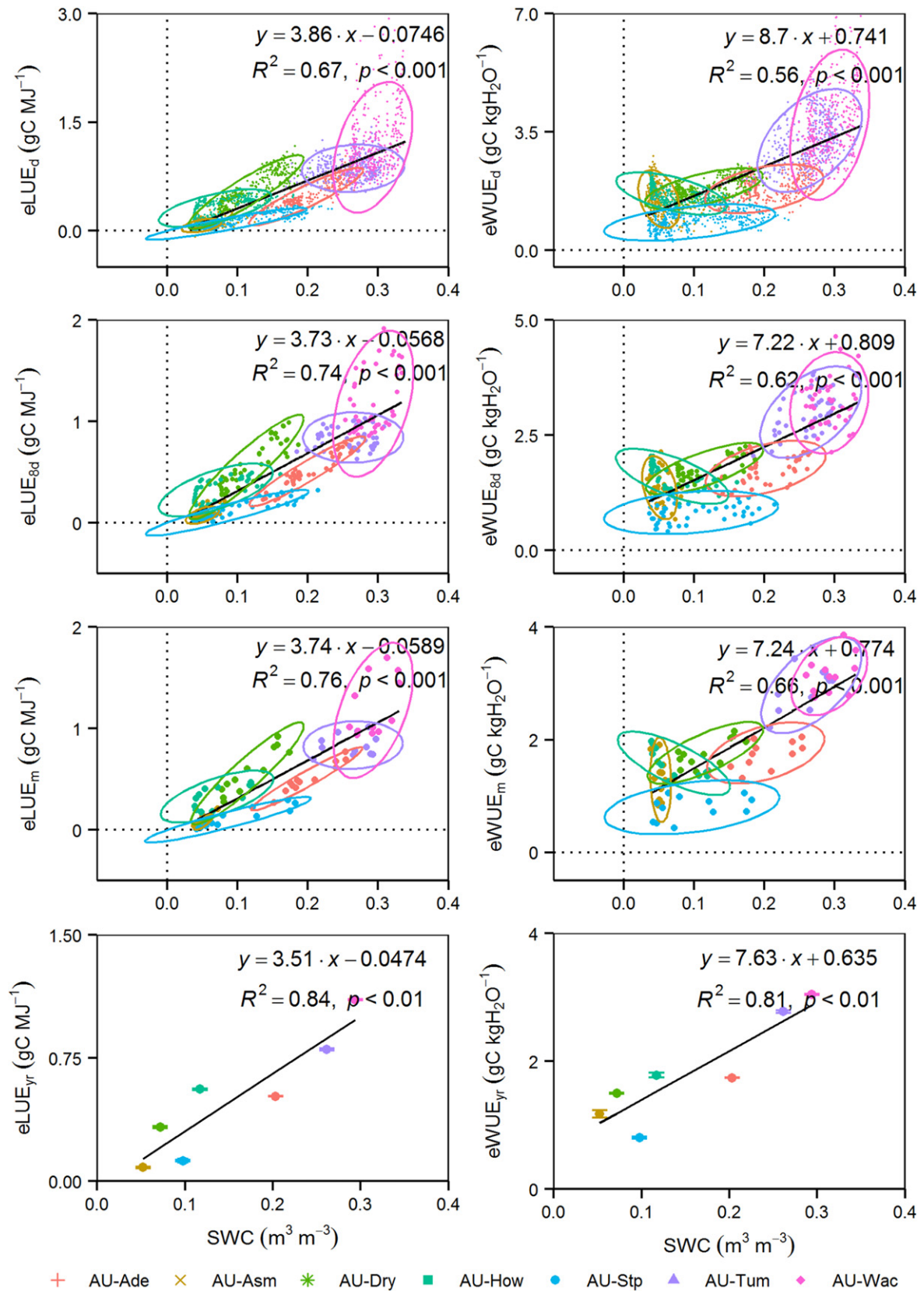


**Figure 3.** Relationships between (left) daily (eLUE<sub>d</sub>), eight day (eLUE<sub>8d</sub>), monthly (eLUE<sub>m</sub>) eLUE and SWC and between (right) daily (eWUE<sub>d</sub>), eight day (eWUE<sub>8d</sub>), monthly (eWUE<sub>m</sub>) eWUE and SWC for seven sites. Ellipses indicate 95% confidence boundaries of eLUE and eWUE. Bars indicate annual standard deviations of eLUE, eWUE or SWC at each site. Also shown are logarithmically fitted functions, coefficients of determination ( $R^2$ ) and  $p$  values.

contrast, eLUE and eWUE in summer showed strong correlation with LAI<sub>max</sub>.

### 3.4. Behavior of eLUE and eWUE in summer and winter

Monthly eLUE and eWUE in summer and winter showed responses to climate variables consistent with the daily/eight-day to annual time-scales (table 1; figure 4) but the correlation between eLUE/eWUE versus SWC in summer became relatively weak compared with VPD and LAI (table 1). During summer, the VPD dependence of eLUE and eWUE were more apparent than dependence on other climate variables and SWC (table 1). By contrast in winter, variations in eLUE and eWUE were less sensitive to VPD (i.e. the fitted slopes in figure 4). Notably, SWC explained slightly more variability in eLUE during winter, than climatic variables in summer, suggesting different controlling factors and/or mechanisms regulating eLUE in contrary hydrothermal conditions.

Seasonal eLUE differed between summer and winter at all sites except three savannas sites (figure 4). Notably, difference of eLUE between summer and winter was significantly large ( $p < 0.001$ ) at the AU-How savannas site. Contrary to AU-How and the grassland, the two EBF sites showed higher eLUE in winter. There was no significant difference of seasonal eWUE at biome scale except EBF. Similar to eLUE, eWUE at the two EBF sites was lower in summer than that in winter.

## 4. Discussion

### 4.1. Relationships between GPP, PAR and ET

Canopy photosynthesis can be linearly related with PAR (McMurtrie and Wang 1993) or show a hyperbolic response function (Ramier *et al* 2009). Hyperbolic responses of canopy photosynthesis to PAR are expected in biomes with low photosynthetic capacity or low LAI (Baldocchi and Amthor 2001), where self-shading within canopies is relatively small, in contrast to biomes with large LAI where light saturation of photosynthesis does not occur so frequently in the lower canopy. Thus, the significant linear correlation of GPP with PAR at EBF sites can be explained by their relatively large LAI (supplementary table S1; figure 1). Thus, these sites are primarily light limited and were not light saturated during the period of measurement. In savannas and the grassland, GPP was not correlated with variations in PAR at these northern tropical sites (figure 1) due to relatively small intra-annual variations in daily average PAR (lower latitude) (supplementary figure S1; figure 1). Seasonal variation in GPP primarily responded to large changes in LAI arising from senescence of the grassy understory as driven by seasonal monsoonal rainfall (Whitley *et al* 2011). Thus it is light interception rather than light supply that limits GPP at these sites.

Coupling of GPP to ET has been observed in many studies (Baldocchi 1994, Beer *et al* 2009), and stems from the intrinsic link between carbon and water fluxes via stomatal

conductance at the leaf level (Beer *et al* 2009). In contrast to reported convergence of annual eWUE across multiple biomes (except for tundra vegetation) (Law *et al* 2002), we only observed similar eWUE values (that is, functional convergence of eWUE) within the savannas (figure 1). Similarly, Ponton *et al* (2006) identified differing eWUE among Douglas-fir forest, aspen forest and grassland within a growing season. However, it is worth noting that the regression slope of GPP against ET in savannas during the dry season (when ET is minimal) was similar to that of forests (figure 1). This is likely to be because ET is driven by C3 trees in the dry season following senescence of the annual grasses. At larger rates of ET during the wet season, C4 grasses dominate the understory and have a larger WUE than C3 plants. Thus, there is some evidence that the eucalypt species examined across temperature and tropical biomes in the current study converged to a common WUE. This result is consistent with the results of O'Grady *et al* (2009), who observed convergence of rates of tree water use within an arid-zone woodland in Australia. Apparent divergence of eWUE between seasons in wet-dry tropical biomes is therefore driven by changes in the relative contributions of upper (C3) and lower (C4) canopies to ET and GPP, rather than changes in functional behavior of the biomes *per se*.

### 4.2. Climate dependence of eLUE and eWUE among biomes

Variations of eLUE were best explained by VPD and SWC while variations of eWUE were best explained by VPD across all time-scales but also well correlated with SWC (table 1). This suggested that VPD co-varied with SWC and water availability was the most influential factor for eLUE/eWUE. Rapid ecosystem transitions that include changes in ecosystem productivity, structure and water cycling can result from long-term climate variations, such as variability in inter-annual precipitation and seasonality of precipitation (Grimm *et al* 2013). Over northern savannas and the grassland, rainfall is the primary environmental controlling factor such that vegetation structure (i.e. tree height and LAI) has adapted to the available resources (Cook *et al* 2002). In contrast, PAR, VPD and air temperature which usually strongly co-vary, were the major drivers of variation in ecosystem productivity in the two temperate forests (Cleverly *et al* 2013, Kanniah *et al* 2011, van Gorsel *et al* 2013). Therefore, climate variables are critical factors that essentially regulate eLUE and eWUE through their long-term influence on ecosystem structure and functioning. Consequently, our results showed a robust intrinsic dependence of eLUE and eWUE on climate across all time-scales.

Several explanations exist for the strong link between eLUE/eWUE and climate. Generally, climatic control of ET and GPP lies somewhere along a continuum between either severe water or energy limitation (Budyko 1974, Whitley *et al* 2011), although temperature also limits productivity in many ecosystems (Churkina and Running 1998). Deficits of radiation, temperature or water that cause a decrease in GPP will lead to lower canopy conductance and ET (Beer *et al* 2009). Most sites in the present study, and particularly



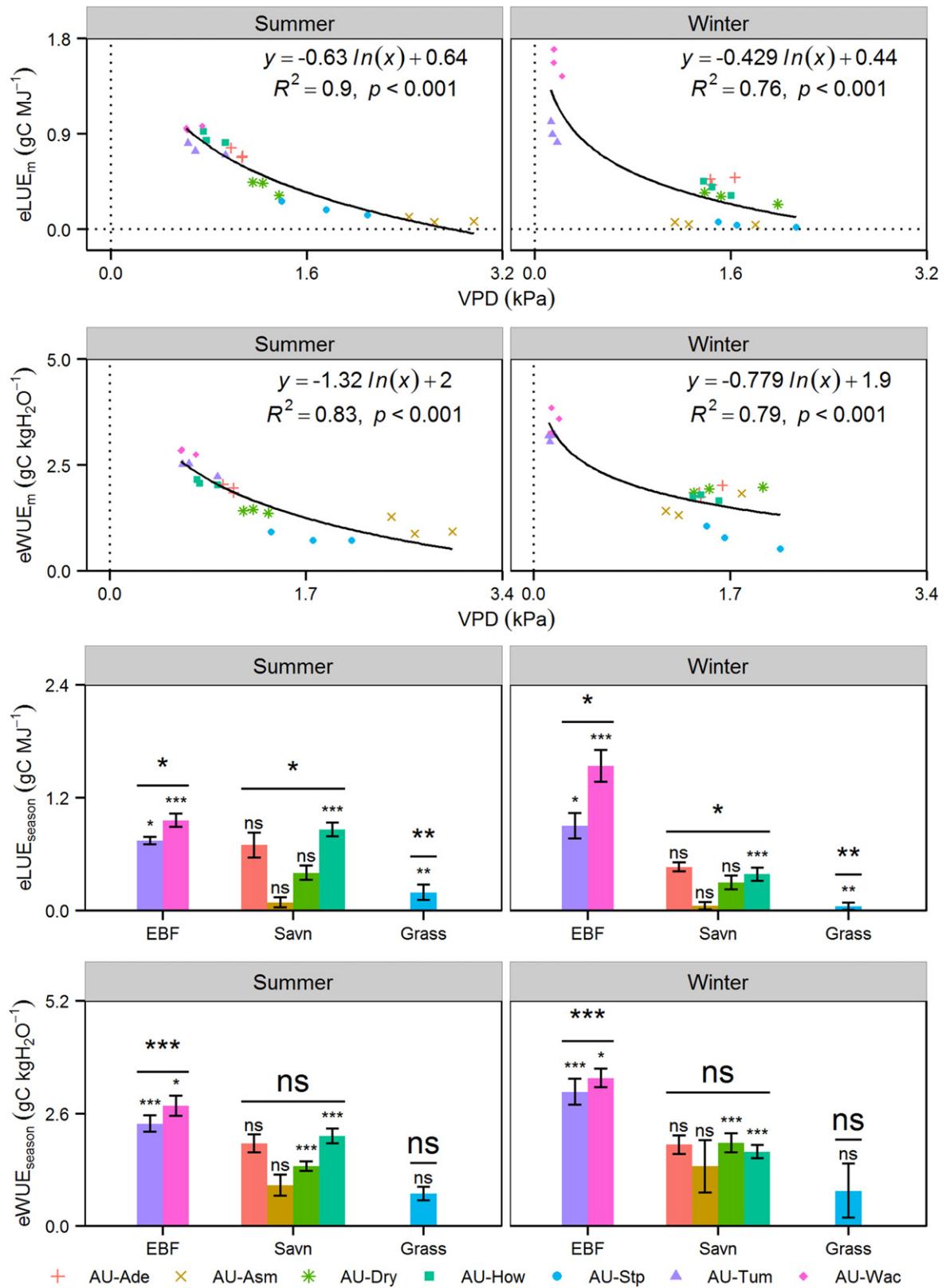


**Figure 4.** Logarithmical relationships between (top two) monthly LUE (eLUE<sub>m</sub>) and VPD and between monthly WUE (eWUE<sub>m</sub>) and VPD in summer and winter, respectively. Comparisons of (bottom two) average seasonal LUE (eLUE<sub>season</sub>) and eWUE (eWUE<sub>season</sub>) for seven sites are also shown in summer and winter, respectively. Error bars indicate the standard deviations of seasonal eLUE or eWUE at each site. ‘\*\*\*’, ‘\*\*’, and ‘\*’ above the error bars of each site indicate significance at 0.001, 0.01, and 0.05 levels, while ‘ns’ represents not significant, based on *t*-test statistics, and these symbols above the horizontal lines represent significance at biome level.

the tropical ones that experience a distinct dry season, did not show evidence of energy supply limitation (as inferred from PAR) at any temporal scales because the range in daily PAR was too small (figure 1). VPD can represent atmospheric evaporative demand and is responsive to patterns of water availability. Increasing VPD leads to reduced GPP through smaller stomatal conductance (Beer *et al* 2009), hence eLUE and eWUE decline with increasing VPD because at low and moderate values of VPD, increasing VPD causes increased ET (Eamus *et al* 2008, Thomas and Eamus 1999, Wharton *et al* 2009) but reduced GPP (table 1; figure 4).

#### 4.3. Seasonal patterns of eLUE and eWUE across biomes

eLUE and eWUE showed significant difference between summer and winter at several sites (figure 4). Seasonal changes in climate variables, SWC and vegetation structure (e.g. LAI<sub>max</sub>) can explain these seasonal similarity or difference. At the EBF sites during winter, GPP increased with PAR. During winter neither temperature nor VPD were supra-optimal for GPP. In contrast, in the summer, increasing PAR was accompanied by either temperature or VPD attaining supra-optimal values, thereby limiting the response of GPP to increased PAR and leading to a smaller eLUE in summer. A similar phenomenon was also found in eWUE. At the EBF sites, both GPP and ET decreased in winter. However, in summer, high VPD and temperature imposed larger limiting effects on GPP than ET, which caused a smaller eWUE in summer. This limiting effect was especially obvious at the AU-Wac site because VPD became increasingly important for GPP during summer compared to winter (Kilinc *et al* 2013). Meanwhile, since both GPP and LAI<sub>max</sub> at AU-Wac were larger in summer whereas the corresponding eLUE was relatively smaller ( $p < 0.01$ ), eLUE was negatively correlated with LAI<sub>max</sub> (supplementary figure S3) as with VPD. At the grassland site, dry winter (supplementary figure S1) caused SWC and LAI to decline significantly compared to summer (data not shown), which decreased canopy photosynthesis and transpiration and further decreased eLUE substantially but not significantly affected eWUE. At AU-How, as a combination of trees and seasonal grass, savannas have larger LAI in summer resulting in a larger GPP. Meanwhile, PAR in winter at AU-How was comparable to that in summer. Consequently, eLUE in summer at this site was larger than that in winter ( $p < 0.001$ ). Similarly, both GPP and ET in winter significantly decreased resulting from senescence of C4 grass and effects of meteorological variables, but the decrease in GPP was stronger than the decrease in ET at AU-How, leading to a smaller eWUE. Contrarily, at AU-Dry the decrease in ET exceeded the decrease in GPP resulting in a larger eWUE in winter. This asynchronous response of GPP and ET to climatic variables or LAI and thus variations of eWUE are in good agreement with previous findings in China (Yu *et al* 2008).

## 5. Conclusions

Climate drivers are critical in regulating water cycling (and consequently SWC) and LAI through their long term influences on ecosystem structure and functioning (Kanniah *et al* 2011). Understanding the spatial patterns of eLUE and eWUE at multiple time-scales and their underlying environmental control mechanisms is of great significance for estimating ecosystem carbon budgets and water carrying capacity under changing hydrothermal conditions (i.e., climate change) (Yu *et al* 2008). In this study, we investigated the relationships between eLUE and eWUE versus climate factors, SWC and vegetation dynamics across diverse climatic regimes with environmental gradients. Across biomes, eLUE and eWUE were tightly and coherently correlated with climate drivers, particularly VPD (and consequently SWC), at multiple time-scales. For any specific biome, eLUE and eWUE were significantly different between summer and winter except eWUE for savannas and the grassland. LAI played an important role in influencing eLUE and eWUE in summer season. Our results provide valuable information for predicting the spatial pattern of eLUE and eWUE at multiple time-scales across Australian biomes. Also this study improves understanding of the responses of ecosystem functional traits to gradients in water availability and temperature, which in turn enables improvements of estimating carbon and water fluxes on a large spatial scale.

## Acknowledgements

This research was supported by an Australian Research Council Discovery Early Career Research Award (project number DE120103022).

## References

- Baldocchi D 1994 A comparative study of mass and energy exchange rates over a closed C<sub>3</sub> (wheat) and an open C<sub>4</sub> (corn) crop: II. CO<sub>2</sub> exchange and water use efficiency *Agric. Forest Meteorol.* **67** 291–321
- Baldocchi D and Amthor J 2001 Canopy photosynthesis: history, measurements, and models *Terrestrial Global Productivity* ed J Roy, B Saugier and H A Mooney (San Diego: Academic) pp 9–31
- Beer C, Ciais P, Reichstein M, Baldocchi D, Law B, Papale D, Soussana J-F, Ammann C, Buchmann N and Frank D 2009 Temporal and among-site variability of inherent water use efficiency at the ecosystem level *Glob. Biogeochem. Cycles* **23** GB2018
- Beer C, Reichstein M, Ciais P, Farquhar G and Papale D 2007 Mean annual GPP of Europe derived from its water balance *Geophys. Res. Lett.* **34** L05401
- Budyko M I 1974 *Climate and Life* (New York: Academic)
- Campos G E P, Moran M S, Huete A, Zhang Y, Bresloff C, Huxman T E, Eamus D, Bosch D D, Buda A R and Gunter S A 2013 Ecosystem resilience despite large-scale altered hydroclimatic conditions *Nature* **494** 349–52

- Churkina G and Running S W 1998 Contrasting climatic controls on the estimated productivity of global terrestrial biomes *Ecosystems* **1** 206–15
- Cleverly J, Boulain N, Villalobos-Vega R, Grant N, Faux R, Wood C, Cook P G, Yu Q, Leigh A and Eamus D 2013 Dynamics of component carbon fluxes in a semi-arid Acacia woodland, central Australia *J. Geophys. Res.: Biogeosciences* **118** 1168–85
- Cook G D, Williams R J, Hutley L, O'Grady A and Liedloff A C 2002 Variation in vegetative water use in the savannas of the North Australian tropical transect *J. Vegetation Sci.* **13** 413–8
- Daubechies I 1990 The wavelet transform, time-frequency localization and signal analysis *IEEE Trans. Inf. Theory* **36** 961–1005
- Ding R, Kang S, Vargas R, Zhang Y and Hao X 2013 Multiscale spectral analysis of temporal variability in evapotranspiration over irrigated cropland in an arid region *Agric. Water Manage.* **130** 79–89
- Eamus D, Hutley L and O'Grady A P 2001 Daily and seasonal patterns of carbon and water fluxes above a North Australian Savanna *Tree Physiol.* **21** 977–88
- Eamus D, Taylor D T, Macinnis-NG C M, Shanahan S and Silva L D 2008 Comparing model predictions and experimental data for the response of stomatal conductance and guard cell turgor to manipulations of cuticular conductance, leaf-to-air vapour pressure difference and temperature: feedback mechanisms are able to account for all observations *Plant Cell Environ.* **31** 269–77
- Eamus D, Cleverly J, Boulain N, Grant N, Faux R and Villalobos-Vega R 2013 Carbon and water fluxes in an arid-zone Acacia Savanna Woodland: an analyses of seasonal patterns and responses to rainfall events *Agric. Forest Meteorol.* **182–183** 225–38
- Farquhar G D, Ehleringer J R and Hubick K T 1989 Carbon isotope discrimination and photosynthesis *Annu. Rev. Plant Biol.* **40** 503–37
- Goetz S and Prince S D 1999 Modelling terrestrial carbon exchange and storage: evidence and implications of functional convergence in light-use efficiency *Adv. Ecol. Res.* **28** 57–92
- Gower S T, Kucharik C J and Norman J M 1999 Direct and indirect estimation of leaf area index,  $f_{APAR}$ , and net primary production of terrestrial ecosystems *Remote Sens. Environ.* **70** 29–51
- Grimm N B *et al* 2013 The impacts of climate change on ecosystem structure and function *Frontiers Ecol. Environ.* **11** 474–82
- Hu Z, Yu G, Fu Y, Sun X, Li Y, Shi P, Wang Y and Zheng Z 2008 Effects of vegetation control on ecosystem water use efficiency within and among four grassland ecosystems in China *Glob. Change Biol.* **14** 1609–19
- Huxman T E, Smith M D, Fay P A, Knapp A K, Shaw M R, Loik M E, Smith S D, Tissue D T, Zak J C and Weltzin J F 2004 Convergence across biomes to a common rain-use efficiency *Nature* **429** 651–4
- Jönsson P and Eklundh L 2004 TIMESAT—A program for analyzing time-series of satellite sensor data *Comput. Geosci.* **30** 833–45
- Kanniah K D, Beringer J and Hutley L 2011 Environmental controls on the spatial variability of savanna productivity in the northern territory, Australia *Agric. Forest Meteorol.* **151** 1429–39
- Kilinc M, Beringer J, Hutley L, Tapper N J and McGuire D A 2013 Carbon and water exchange of the world's tallest angiosperm forest *Agric. Forest Meteorol.* **182** 215–24
- Lafont S, Kergoat L, Dedieu G, Chevillard A, Karstens U and Kolle O 2002 Spatial and temporal variability of land CO<sub>2</sub> fluxes estimated with remote sensing and analysis data over Western Eurasia *Tellus B* **54** 820–33
- Law B, Falge E, Gu L V, Baldocchi D, Bakwin P, Berbigier P, Davis K, Dolman A, Falk M and Fuentes J 2002 Environmental controls over carbon dioxide and water vapor exchange of terrestrial vegetation *Agric. Forest Meteorol.* **113** 97–120
- Li S G, Eugster W, Asanuma J, Kotani A, Davaa G, Oyunbaatar D and Sugita M 2008 Response of gross ecosystem productivity, light use efficiency, and water use efficiency of mongolian steppe to seasonal variations in soil moisture *J. Geophys. Res.: Biogeosciences (2005–2012)* **113** G01019
- McMurtrie R and Wang Y P 1993 Mathematical models of the photosynthetic response of tree stands to rising CO<sub>2</sub> concentrations and temperatures *Plant Cell & Environ.* **16** 1–13
- Niu S, Xing X, Zhang Z, Xia J, Zhou X, Song B, Li L and Wan S 2011 Water-use efficiency in response to climate change: from leaf to ecosystem in a temperate steppe *Glob. Change Biol.* **17** 1073–82
- O'Grady A, Cook P, Eamus D, Duguid A, Wischusen J, Fass T and Worldege D 2009 Convergence of tree water use within an arid-zone woodland *Oecologia* **160** 643–55
- Polley H W, Phillips R L, Frank A B, Bradford J A, Sims P L, Morgan J A and Kiniry J R 2011 Variability in light-use efficiency for gross primary productivity on Great Plains grasslands *Ecosystems* **14** 15–27
- Ponton S, Flanagan L B, Alstad K P, Johnson B G, Morgenstern K, Kljun N, Black T A and Barr A G 2006 Comparison of ecosystem water-use efficiency among Douglas-fir forest, aspen forest and grassland using eddy covariance and carbon isotope techniques *Glob. Change Biol.* **12** 294–310
- Rahman A, Sims D, Cordova V and El-Masri B 2005 Potential of MODIS EVI and surface temperature for directly estimating per-pixel ecosystem C fluxes *Geophys. Res. Lett.* **32** L19404
- Ramier D, Boulain N, Cappelaere B, Timouk F, Rabanit M, Lloyd C R, Boubkraoui S, Métayer F, Descroix L and Wawrzyniak V 2009 Towards an understanding of coupled physical and biological processes in the cultivated Sahel–1. Energy and water *J. Hydrol.* **375** 204–16
- Scanlon T M and Albertson J D 2001 Turbulent transport of carbon dioxide and water vapor within a vegetation canopy during unstable conditions: identification of episodes using wavelet analysis *J. Geophys. Res.: Atmospheres (1984–2012)* **106** 7251–62
- Schwalm C R, Black T A, Amiro B D, Arain M A, Barr A G, Bourque C P-A, Dunn A L, Flanagan L B, Giasson M-A and Lafleur P M 2006 Photosynthetic light use efficiency of three biomes across an east–west continental-scale transect in Canada *Agric. Forest Meteorol.* **140** 269–86
- Stoy P C, Katul G G, Siqueira M B, Juang J-Y, McCarthy H R, Kim H-S, Oishi A C and Oren R 2005 Variability in net ecosystem exchange from hourly to inter-annual time scales at adjacent pine and hardwood forests: a wavelet analysis *Tree Physiol.* **25** 887–902
- Thomas D and Eamus D 1999 The influence of predawn leaf water potential on stomatal responses to atmospheric water content at constant C<sub>i</sub> and on stem hydraulic conductance and foliar ABA concentrations *J. Exp. Bot.* **50** 243–51
- Torrence C and Compo G P 1998 A practical guide to wavelet analysis *Bull. Am. Meteorol. Soc.* **79** 61–78
- Turner D P, Urbanski S, Bremer D, Wofsy S C, Meyers T, Gower S T and Gregory M 2003 A cross-biome comparison of daily light use efficiency for gross primary production *Glob. Change Biol.* **9** 383–95
- van Gorsel E *et al* 2013 Primary and secondary effects of climate variability on net ecosystem carbon exchange in an evergreen Eucalyptus forest *Agric. Forest Meteorol.* **182–183** 248–56
- Wharton S, Schroeder M, Bible K and Falk M 2009 Stand-level gas-exchange responses to seasonal drought in very young versus old Douglas-fir forests of the Pacific Northwest, USA *Tree Physiol.* **29** 959–74

- Whitley R J, Macinnis-Ng C M O, Hutley L B, Beringer J, Zeppel M, Williams M, Taylor D and Eamus D 2011 Is productivity of mesic savannas light limited or water limited? Results of a simulation study *Glob. Change Biol.* **17** 3130–49
- Xiao X, Zhang Q, Hollinger D, Aber J and Moore B III 2005 Modeling gross primary production of an evergreen needleleaf forest using MODIS and climate data *Ecol. Appl.* **15** 954–69
- Yu G, Song X, Wang Q, Liu Y, Guan D, Yan J, Sun X, Zhang L and Wen X 2008 Water-use efficiency of forest ecosystems in eastern China and its relations to climatic variables *New Phytologist* **177** 927–37



## Intrinsic climate dependency of ecosystem light and water-use-efficiencies across Australian biomes

This content has been downloaded from IOPscience. Please scroll down to see the full text.

2014 Environ. Res. Lett. 9 104002

(<http://iopscience.iop.org/1748-9326/9/10/104002>)

View [the table of contents for this issue](#), or go to the [journal homepage](#) for more

### Download details:

IP Address: 138.25.85.133

This content was downloaded on 28/10/2014 at 01:05

Please note that [terms and conditions apply](#).

## Supplementary Information

### 1. Eddy Covariance Flux Sites

The dominant woody species differ among the sites. The AU-How and AU-Dry sites are *Eucalyptus tetradonta*/*Eucalyptus miniata* dominated savannas (tree height 12 m), which are widely distributed across tropical Australia (Hutley *et al.*, 2011). The AU-Ade site is dominated by *Eucalyptus tectifica* and *Corymbia latifolia* (tree height 16 m) as a result of the finer textured and poorly drained soils. The canopy dominant tree species at the AU-Asm site is the N<sub>2</sub> fixing species *Acacia aneura*, which is 6.5 m tall on average. Each of these sites (AU-How, AU-Dry, AU-Ade and AU-Asm) are classified as savanna, a biome defined by a discontinuous tree canopy with a grassy understory (Eamus & Prior, 2001) experiencing seasonality in rainfall. The grassland AU-Stp is dominated by Mitchell grass within an extensive tussock grassland ecosystem that occurs on heavily cracking clay soils. The AU-Tum site is classified as a wet sclerophyllous forest and is dominated by *Eucalyptus delegatensis* (tree height 40 m). The AU-Wac site is an 300-year-old growth stand dominated by *Eucalyptus regnans* (tree height 75 m) with a temperate rainforest understory consisting of *Pomaderris aspera* and *Olearia argophylla* (tree height 10-18 m) (Kilinc *et al.*, 2013).

### 2. Flux Gap Filling and Partitioning method

Half-hourly carbon and water fluxes, rainfall, air and soil temperature, soil water content, absolute humidity, downward shortwave radiation and net radiation were measured using an eddy covariance system and associated meteorological and soil moisture sensors installed at each site. PAR and ET were calculated as downward shortwave radiation (unit: W m<sup>-2</sup>) times 0.5 and latent heat flux (unit: W m<sup>-2</sup>) divided by the latent heat of vaporization (2450 J g H<sub>2</sub>O<sup>-1</sup>), respectively. Water and CO<sub>2</sub> fluxes were processed through OzFlux level 2 (i.e., QA/QC) and level 3 (e.g. rotation, correction for frequency attenuation, and density-flux

(WPL) corrections) using standardized methodology (Eamus *et al.*, 2013). The post processing of the quality controlled data to fill gaps in meteorology, soil moisture and fluxes as well as partitioning NEE into GPP and ecosystem respiration was performed using the Dynamic INtegrated Gap filling and partitioning for Ozflux (DINGO) system. The system was coded in Python and consisted of modules to gap fill meteorological variables (air temperature, specific humidity, wind speed and barometric pressure) using nearby Bureau of meteorology ([www.bom.gov.au](http://www.bom.gov.au)) automatic weather stations that were correlated and corrected to tower observations. All radiation streams were gap-filled using a combination of MODIS albedo products (MCD43 BRDF-Albedo suite) and Bureau of Meteorology (BoM) gridded global solar radiation and gridded daily meteorology from the Australian Water Availability Project data set (BoM AWAP) (Jones *et al.*, 2009). Precipitation was gap-filled using either nearby BoM stations or BoM AWAP. Soil temperature and moisture were filled using the BIOS2 land surface model (Haverd *et al.*, 2013) run for each site forced with BoM AWAP data. Gap filling of fluxes were performed using an Artificial Neural Network (ANN) model using a multilayer network of full connectivity following Beringer *et al.* (2007). Training was done using gradient information in a truncated Newton algorithm. NEE and the fluxes of sensible, latent and ground heat fluxes were modelled using the ANN with incoming solar radiation, VPD, soil moisture content, soil temperature, wind speed and MODIS EVI as inputs. The Ustar threshold for each site was determined following (Reichstein *et al.*, 2005) and night time observations below the Ustar threshold were replaced with ANN modelled values of ecosystem respiration using soil moisture content, soil temperature, air temperature and MODIS EVI as inputs. The ANN model for ecosystem respiration was applied to daylight periods to estimate daytime respiration and GPP was calculated as the difference between net ecosystem exchange and ecosystem respiration.

**Table S1.** La Thuile code, site name, latitude (Lat), longitude (Long), year of observations, altitude (Alt), biomes (Evergreen Broadleaf Forests, EBF; Savannas, Savn; Grasslands, Grass), mean maximum annual temperature ( $T_{\max}$ ), mean minimum annual temperature ( $T_{\min}$ ), mean annual precipitation (MAP), mean annual minimum leaf area index ( $LAI_{\min}$ ) and mean annual maximum LAI ( $LAI_{\max}$ ) during observation intervals for the study sites.

La Thuile code	Site name	Lon	Lat	Year	Alt (m)	Biomes	$T_{\max}$ (°C)	$T_{\min}$ (°C)	MAP (mm)	$LAI_{\min}$ - $LAI_{\max}$ ( $m^2/m^2$ )
AU-How	Howard Springs	131.15 E	12.50 S	2004-2008	64	Savn	39.3	12.2	1201	1.23-2.16
AU-Ade	Adelaide River	131.12 E	13.08 S	2007-2009.05	90	Savn	38.0	11.7	1852	0.73-2.04
AU-Dry	Dry River	132.37 E	15.26 S	2009-2012.09	175	Savn	40.6	8.9	995	1.03-1.66
AU-Stp	Sturt Plains	133.35 E	17.15 S	2008-2012	250	Grass	42.7	6.2	695	0.38-1.03
AU-Asm	Alice Springs	133.25 E	22.28 S	2010.09-2013.09	606	Savn	40.8	0.2	335	0.27-0.47
AU-Tum	Tumbarumba	148.15 E	35.66 S	2008-2012	1200	EBF	29.3	-2.9	1000	4.06-5.58
AU-Wac	Wallaby Creek	145.19 E	37.43 S	2006-2008	720	EBF	33.1	-0.1	1595	0.98-5.01



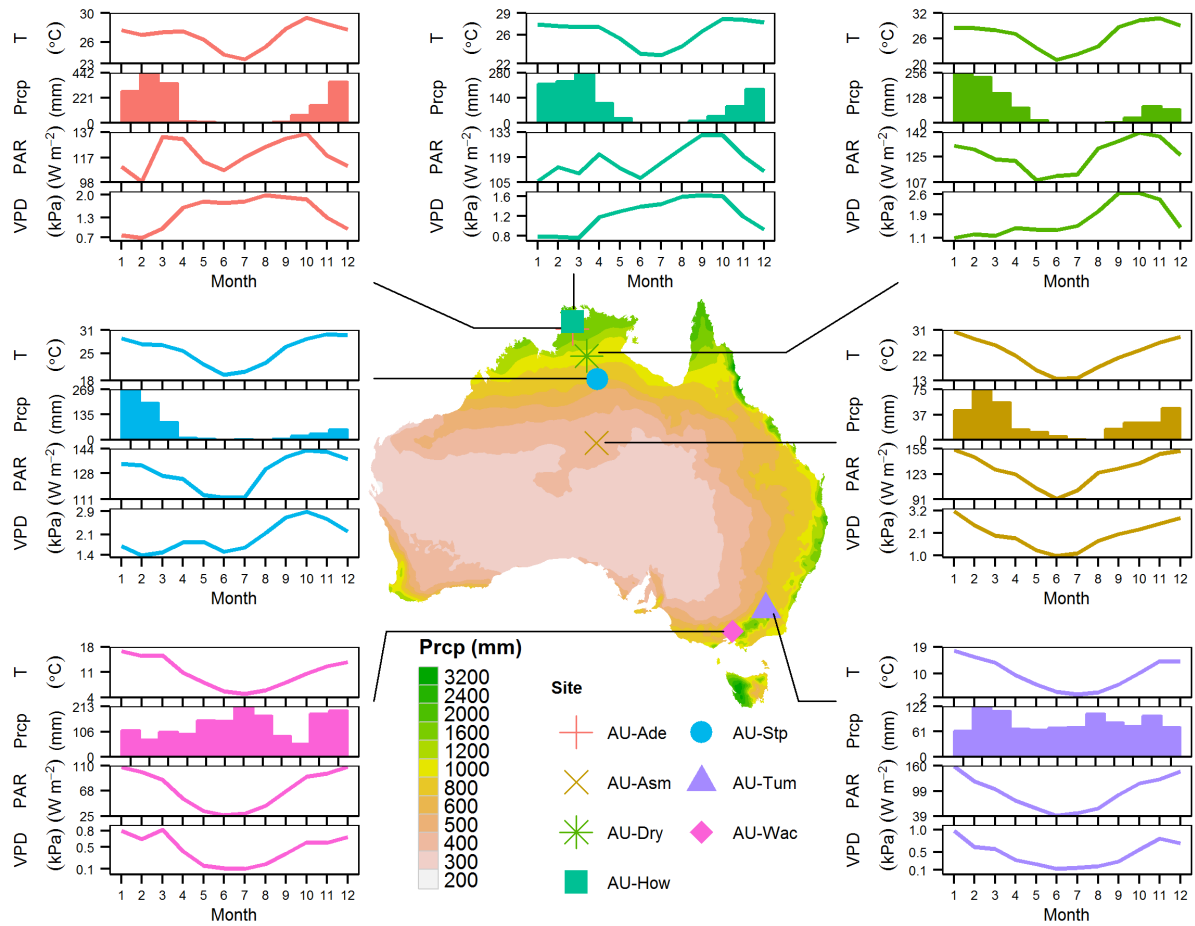


**Figure S1.** Average annual precipitation contour map of Australia in 30 years from 1976 to 2005 (statistics by Bureau of Meteorology, Australia), spatial distribution of selected sites and average monthly climate over the respective observation periods for each site (Table 1). T indicates temperature, Prctp indicates precipitation, PAR indicates photosynthetically active radiation, and VPD indicates the vapor pressure deficit.

### 3. Wavelet transform example

The Morlet mother wavelet function can be represented as:

$$\psi_0(\eta) = \pi^{-1/4} e^{i\omega_0\eta} e^{-\eta^2/2} \quad (1)$$

where  $\omega_0$  is the frequency and is taken as 6 to make above function have zero mean and be localized in both time and frequency space. To ensure the wavelet transform at different scales are comparable to each other and the transforms of other time series, the  $\psi_0(\eta)$  wavelet function at each scale  $s$  is normalized as:

$$\psi(\eta) = \left(\frac{\delta t}{s}\right)^{1/2} \psi_0(\eta) \quad (2)$$

where  $\delta t$  is the time step of the time series. Then the continuous wavelet transform of a discrete time series  $x_n$  is the convolution of  $x_n$  with a scaled and translated Morlet mother wavelet:

$$W_n(s) = \sum_{t=0}^{N-1} x_t \psi^* \left[ \frac{(t-n)\delta t}{s} \right] \quad (3)$$

where  $n$  indicates the localized time index,  $N$  is the number of  $x_n$  and  $(*)$  indicates the complex conjugate. The scale  $s$  is usually given as fractional powers of two:

$$s_j = s_0 2^{j\delta j}, j = 0, 1, \dots, J \quad (4)$$

where  $s_0$  is the smallest resolvable scale and generally taken to be  $2\delta t$ ,  $\delta j$  indicates the scale sampling step and given to be 1/12 here and  $J = \delta j^{-1} \log(2, N\delta t / s_0)$  indicates the number of scales. Then the reconstructed time series at scale  $k$  is the sum of the real part of the wavelet transform over  $k$  to  $J$  scales:

$$x_{n,k} = \frac{\delta j \delta t^{1/2}}{C_\delta \psi_0(0)} \sum_{j=k}^J \frac{R\{W_n(s_j)\}}{s_j^{1/2}} \quad (5)$$

where  $R$  indicates the real part of complex and  $C_\delta$  is a constant of 0.776.

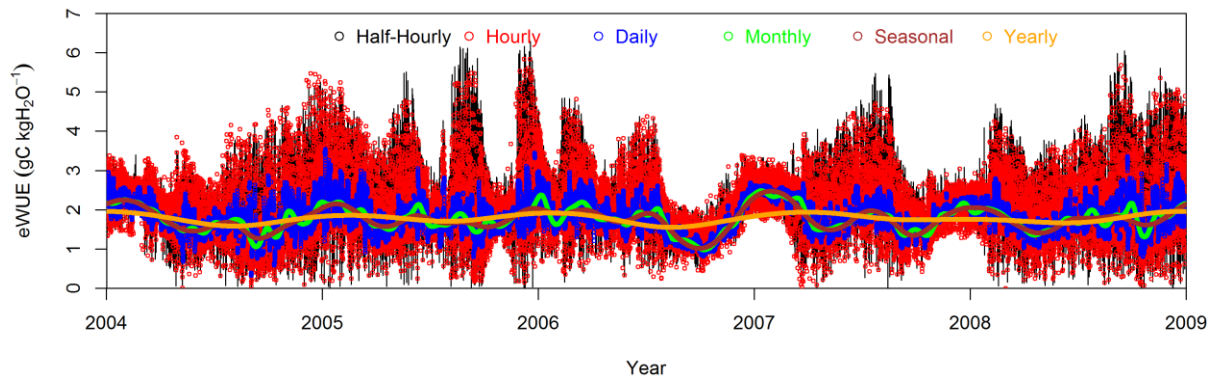


**Figure S2.** eWUE reconstruction at hourly, daily, monthly, seasonal and yearly scales using the wavelet transform at the Howard Springs site from 2004 to 2008. The reconstructed time series removes the higher frequency information in lower scales.

#### 4. Relationships of eLUE and eWUE to $LAI_{max}$

Correlations between  $LAI_{max}$  with eLUE and eWUE among biomes were not found within all sites. In contrast, for example, there was a significant decrease in eLUE and eWUE with  $LAI_{max}$  increasing at AU-Wac site. Similar to climate variables, the correlation among biomes became stronger as time-scale increased.

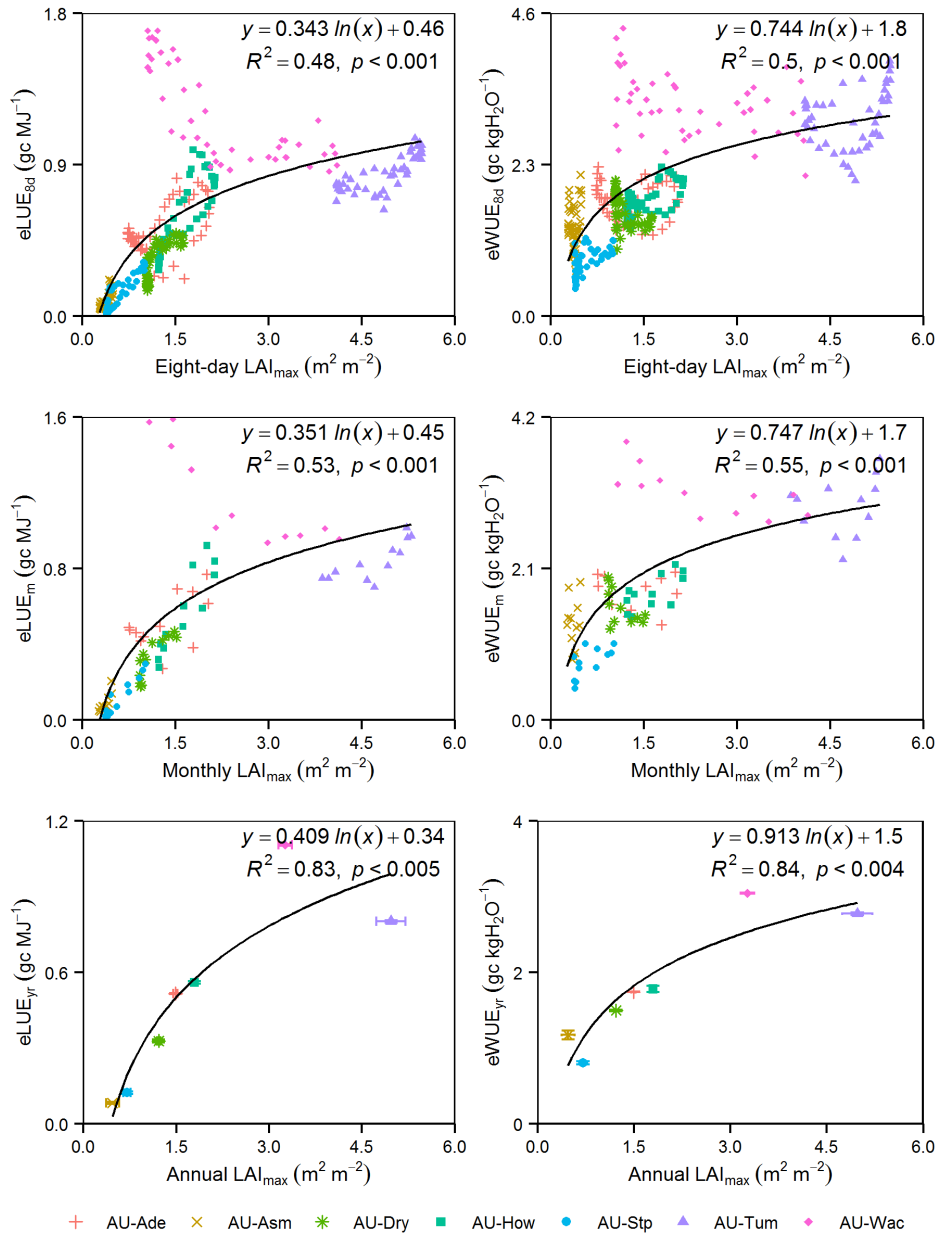


**Figure S3.** Relationships between (left) eight day (eLUE<sub>8d</sub>), monthly (eLUE<sub>m</sub>) and yearly (eLUE<sub>yr</sub>) eLUE and mean maximum LAI (LAI<sub>max</sub>) and between (right) eight day (eWUE<sub>8d</sub>), monthly (eWUE<sub>m</sub>) and yearly (eWUE<sub>yr</sub>) eWUE and LAI<sub>max</sub> for seven sites. Bars indicate standard annual deviations of eLUE, eWUE or LAI<sub>max</sub>. Also shown are logarithmically or linearly fitted functions, coefficients of determination ( $R^2$ ) and  $p$  values.



## References

- Beringer J, Hutley L, Tapper N J and Cernusak L A 2007 Savanna fires and their impact on net ecosystem productivity in North Australia *Glob. Change Biol.* **13** 990-1004
- Eamus D, Cleverly J, Boulain N, Grant N, Faux R and Villalobos-Vega R 2013 Carbon and water fluxes in an arid-zone *Acacia* savanna woodland: An analyses of seasonal patterns and responses to rainfall events *Agric. Forest Meteorol.* **182–183** 225-38
- Eamus D and Prior L 2001 Ecophysiology of trees of seasonally dry tropics: comparisons among phenologies *Adv. Ecol. Res.* **32** 113-97
- Haverd V, Raupach M, Briggs P, Canadell J, Isaac P, Pickett-Heaps C, Roxburgh S, van Gorsel E, Viscarra Rossel R and Wang Z 2013 Multiple observation types reduce uncertainty in Australia's terrestrial carbon and water cycles *Biogeosciences* **10** 2011-40
- Hutley L, Beringer J, Isaac P R, Hacker J M and Cernusak L A 2011 A sub-continental scale living laboratory: Spatial patterns of savanna vegetation over a rainfall gradient in northern Australia *Agric. Forest Meteorol.* **151** 1417-28
- Jones D A, Wang W and Fawcett R 2009 High-quality spatial climate data-sets for Australia *Australian Meteorological and Oceanographic Journal* **58** 233
- Kilinc M, Beringer J, Hutley L, Tapper N J and McGuire D A 2013 Carbon and water exchange of the world's tallest angiosperm forest *Agric. Forest Meteorol.* **182** 215-24
- Reichstein M, Falge E, Baldocchi D, Papale D, Aubinet M, Berbigier P, Bernhofer C, Buchmann N, Gilmanov T and Granier A 2005 On the separation of net ecosystem exchange into assimilation and ecosystem respiration: review and improved algorithm *Glob. Change Biol.* **11** 1424-39